ISSN No:-2456-2165

Power Generation System with Low Enthalpy Geothermal Source:Kalina Cycle

J. M. Shehata
Mechanical Department, Vocational Training Institute,
The Public Authority for Applied Education and Training,
Kuwait City, Kuwait

Abstract:- The purpose of this research is to investigate the feasibility of utilizing low enthalpy geothermal energy in a thermal power system. The Kalina cycle is suggested in this research and will be evaluated in the light of energy and exergy analysis. Binary NH_3/H_2O mixture will be utilized as a working fluid. Through a parametric study, NH_3/H_2O mixture strength and geothermal source temperature will be varied and tested against the performance of Kalina system. A comparison with conventional Rankine cycle performance, working at the same boundary conditions, will be also performed.

Results showed that as NH_3/H_2O mixture strength increases, both heat transfer area for condenser and evaporator are increases, and the required heat transfer area for the condenser is greater than evaporator. The net cycle electrical power increases with the increase of NH_3/H_2O mixture strength. Results also showed that as geothermal working fluid temperature increases the net cycle electrical power increases, where the heat transfer area for the evaporator sharply decrease. As per exergy destruction, results showed that the highest value of exergy destruction occurred in the turbine followed by the evaporator, where the lowest values occur in the condenser and the separator.

Keywords:- *Geothermal Energy, Kalina Cycle, NH_3/H_2O Mixture, Exergy Destruction.*

I. INTRODUCTION

Energy resources can be classified into three main categories; fossil, renewable and nuclear energy. Renewable energy is considered as one of the most clean and sustainable resources with negligible levels of emission. The renewable energy sources are expected to provide 20 to 40% of the primary energy in 2050, renewable energy sources can exist in several forms such as solar, biomass, hydropower, wind, tidal and geothermal [1].

Geothermal energy has a relatively long history of industrial applications, geothermal power plant (250 kW) was invented by Prince Piero Ginori Conti in Italy in 1904. Today, around 24 countries utilizing geothermal energy for power production, Table 1. The installed electrical capacity reached 3,086 MW in US, and a country such as Iceland derives 25% of electricity and 90% of heating needs from geothermal resources [2].

The remarkable impact of geothermal energy is highly appreciated in electric generation industry. The geothermal fluid, named liquid brine, is extracted from hydrothermal reservoir, liquid brine characterized with low enthalpy, rich minerals and high level of salinity. Unfortunately, it contains hydrogen sulfide and mercury, so special treatment should be considered during operation [3].

Several types of geothermal systems can be exploited: convective system (called hydrothermal), enhanced geothermal system (EGS), conductive sedimentary system, hot water produces from oil and gas fields, geo pressured system and magma bodies [4]. As per temperature scale classification, geothermal resources can be classified into low (<90^{o}C), intermediate (90-150^{o}C) and high enthalpy resources.

Lee [5], proposed specific exergy index SExI, with three classifications; low, medium and high-quality geothermal resources, where

$$\mathrm{SExI} = \frac{h_{brine} - 273.16\, s_{brine}}{1192}$$

where h_{brine} is the enthalpy of the brine (kJ/kg) and s_{brine} is the entropy of the brine (kJ/kgK). SExI is a straight line on h-s plot of the Mollier diagram. Straight lines of SExI=0.5 and 0.05 can therefore be drawn on this diagram and used as a map for classifying geothermal resources by taking into account the following:

SExI < 0.05 for low quality geothermal resources
0.05 ≤ SExI < 0.5 for medium quality geothermal resources
SExI ≥ 0.5 for high quality geothermal resources

where the demarcation limits for these indices are exergies of saturated water and dry saturated steam at 1 bar.

The global installed geothermal energy capacity reaches 10,715 MW in year 2010, which shows a 20% increase compared to year 2005 (8,933 MW). In addition, the number of states that use geothermal energy increase significantly from 47 countries in year 2007 to 70 countries in 2010, [6].

II. KALINA CYCLE

There are three basic types of geothermal power stations: (a) Dry steam station, where hot steam typically above 235^{o}C, in which steam directly used to run different types of generators, (b) Flash steam station, where the steam pressure is high and temperature is above 182^{o}C, hot water can be pumped from reservoir to power station, and (c) Binary cycle, where hot water characterized with low temperature(s), where in binary cycle two working fluids are utilized; such as water and ammonia, one application of binary cycle is Kalian cycle, [6].

In the last two decades Kalina cycle was proposed industrially to improve power plant efficiency. Kalina cycle is considered as a novel and promising cycle that can convert low energy sources into useful power. It is characterized with an efficient usage of various forms of low enthalpy heat sources such as; gas turbines exhaust gas, exhaust from industrial plants and geothermal sources.

Kalina cycle is a modified type of Rankine cycle with distillation (separator) and absorption (recuperator) components; it was invented by Alex Kalina in 1980's, Figure 1. In Kalina cycle, a mixture of NH_3/H_2O is used as a working fluid, the strength of NH_3/H_2O mixture is intentionally varied across the entire cycle, one major advantage of NH_3/H_2O strength variation is that mixture can boil and condense over a wide range of temperature(s), Figure 2. Since NH_3/H_2O mixture is a non-azeotropic mixture, boiling phenomenon can occurs under a non isothermal process; such *unique* phenomenon tends to increase the temperature of heat addition and reduces the temperature of heat rejection. Hence, the variation(s) in mixture phase provides a noticeable enhancement in cycle thermal efficiency. When NH_3/H_2O mixture heated at low temperature, and due to the chemical characteristics of NH_3, volatile ammonia tends to vaporize before water at different values of temperatures. On the other side, H_2O tends to condense first when NH_3/H_2O mixture cooled down. One should noticed that NH_3 has a lower values of boiling/condensation temperatures compared to pure H_2O, and NH_3 has a lower value of viscosity, so small pipe diameter can be utilized in cycle without any precautions.

Kalina cycle is a simple, friendly, safe and low capital cost type. It can operate with a conventional steam turbine (50-100 MW). Examples of Kalina systems that been installed commercially; (a) 1.3 MW plant in Kashima, Japan and (b) 1.8 MW plant in Husavik, Iceland [3].

As per comparing Kalina with conventional Rankine cycle, studies showed that Kalina cycle showed advantages compared to conventional Rankine cycle, when both cycles operate at the same source and sink temperatures, Kalina cycle shows a 10 to 20% improvement in thermal efficiency. In Kalina cycle the conventional boiler is replaced by vapor generator, and the condenser by distillation/condensation system. The distillation/condensation system consists of low-pressure condenser, vaporizer, pre-heater and a pump. The vapor turbine is usually made of 316 stainless steel, so it can withstand the corrosion effect of NH_3/H_2O mixture [7].

III. LITERATURE REVIEW

Several investigators studied the advantages and the performance of Kalina cycle in terms of energy and exergy analysis [8-13].

Murugan and Subbarao [14] investigate the effectiveness of utilizing low-grade steam in a Kalina cycle. Their results showed that, at optimized condition, 14.7% more power can be achieved compared to Rankine cycle, and 2.1% more efficient compared to Rankine. As per exergy destruction, Kalina cycle showed a reduction of 2.2% compared to Rankine cycle. Also, in other work [15], they proposed a combined cycle operating on a condensing mode, where water is used in topping cycle and NH_3/H_2O mixture in bottom cycle. Their results showed that combined cycle is 4% more efficient than Rankine cycle, and using bottoming cycle provides flexibility to raise boiler pressure, reduce energy losses in the condenser and achieve higher power output with low grade steam.

Marston [16], performed a parametric analysis using Kalina cycle, computer models been used to optimize a simplified form of the cycle to compare results with published complex version. Several thermodynamic property diagrams been evaluated, in addition of cycle efficiency and exergy fraction calculations.

Lu and Goswami [17], proposed new combined power/refrigeration cycle using NH_3/H_2O mixture as a working fluid, the aim of their research was to produce both power and refrigeration. The cycle was optimized for maximum second law efficiency.

Nasruddin et al. [18], investigated the utilization of waste heat produces by power plant; they suggested Kalina cycle as an option to generate additional power from waste heat or from low temperature geothermal resources. The numerical study was performed using Cycle Tempo 5.0 simulation software. A parametric study was performed on Kalina cycle 34, the study covered energy, exergy and optimization analysis. Their results showed that the maximum efficiency and the power output can be achieved at 78% NH_3/H_2O mixture strength value.

Lolos and Rogdakis [19], investigate Kalina cycle operating at low pressure levels (0.2 to 4.5 bar) and low "maximum" temperature (130^{o}C), they presented a hybrid absorption power cycle, based on Kalina cycle. The working fluid mixture was NH_3/H_2O (95%); mixture vaporized using flat solar collectors in addition to external low temperature heat source.

A parametric analysis was conducted to specify the optimum values of main parameters; low pressure, low temperature, vapor mass fraction with respect to efficiency and work output.

Valdimarsson and Eliasson [20] investigated factors that influence the economics of Kalina cycle, a comparison was performed between Kalina and Organic power cycle. Operational parameters were considered in his study; source inlet temperature, mixture strength and pressure been varied. Results showed that Kalina cycle has a similar installed cost compared to a high-power organic power cycle.

Dejfors and Svedberg [21], performed exergy analysis on Kalina power cycle, their results showed that Kalina cycle has exergy losses in the condensers and higher exergy losses in heat exchanger compared with conventional Rankine cycle.

Vidal et al. [22], performed exergy analysis on a new cycle that been produces power and cooling simultaneously, the new cycle was able to operate using low temperature heat source, and produce both power and cooling with NH3/H_2O as a working fluid. They were able to indicate the cycle effectiveness and most of irreversible processes through exergy analysis.

IV. CYCLE MODELING

A steady state component model for Kalina cycle is developed in terms of mass, energy and exergy. The calculations were carried out using IPSEpro software (version 4). The following assumptions are considered during modeling and calculations:

- ✓ Kinetic and potential energy changes are neglected.
- ✓ The isentropic efficiency of turbine and pump are 0.85 and 0.75, respectively.
- ✓ Turbine inlet conditions are 19.8 bar and 88^{o}C.
- ✓ Constant overall heat transfer coefficient for condenser and evaporator.
- ✓ NH_3/H_2O mixture leaves the condenser as a saturated liquid.
- ✓ All heat exchangers are considered as shell and tube counter flow heat exchangers.
- ✓ The chemical exergy type been neglected.
- ✓ Kalina cycle model is presented in Table 2.

V. RESULTS

A. NH_3/H_2O phase diagram

The Binary NH_3/H_2O mixture had been used in refrigeration industry for long time as a working fluid. Henry stated that “a mixture of two fluids behave like a totally new fluid” where Maack and Valdimarsson stated “there is no black magic behind Kalina technology, it is pure thermodynamic” [23]. The NH_3/H_2O mixture characterized with several different features compared to pure NH_3 or H_2O; (a) it is characterized with a variable range of boiling/condensation temperature(s), (b) the thermo-physical properties of the mixture can be altered via changing mixture strength, (c). mixture temperature can be increased or decreased without a change in the value of heat content, and finally (d) solution of NH_3/H_2O mixture have very low freezing temperature. As an example, 25% NH_3/H_2O mixture has a freezing temperature of -51^{o}C [7].

Figure 2 shows the phase diagram of NH3/H2O mixture, one should noticed that evaporation and condensation occurred at constant pressure, at the same time at variable temperature(s), in another word the NH3/H2O mixture has the ability, through an isobaric process, to evaporate and condense at variable values of temperature(s). Such phenomenon contradicts the behavior of evaporation/condensation processes for pure substance (such as pure NH3 or H2O).

Figure 2 also shows the evaporation temperature (bubble temperature) and condensation temperature (dew temperature) as a function of NH3/H2O mixture strength and pressure. Results showed that at elevated values of NH_3/H_2O mixture strength, say 80%, the saturated temperature for both evaporation and condensation processes are low compared to low value of NH_3/H_2O mixture strength (20%), with such phenomenon, changing mixture strength provides another degree of freedom to manipulate pressure [6].

Figure 3 shows the effect of NH_3/H_2O mixture pressure on boiling and condensation temperatures. Results showed that as mixture pressure increases, both boiling and condensation temperatures increase.

B. Energy and Exergy Analysis

Figure 4 shows the effect of NH_3/H_2O mixture strength on heat transfer area; for condenser and evaporator. Results showed that as NH_3/H_2O mixture strength increases heat transfer area for both heat exchangers increases, meantime, one should notice that the heat transfer area increase for evaporator is less compared to the sharp increase of condenser heat transfer area. Calculations showed that as NH_3/H_2O mixture strength increases, $LMTD_{evap}$ was constant at 3.0 K, where $LMTD_{cond}$ was decreased from 3.1 to 2.1 when mixture strength increases from 0.87 to 0.91. The reason behind this reduction in temperature difference is due to the fact that increasing mixture strength reduces the condensation temperature of mixture as shown in Figure 1, and since cooling water temperature was kept constant (seawater temperature), the net temperature difference between the mixture and cooling water is decreased. Heat transfer coefficient is also considered as constant, so more heat transfer area is required for the condenser. Results showed about 95% increases in condenser heat transfer area.

Figure 5 shows the effect of NH_3/H_2O mixture strength on Kalina net electric power output and thermal efficiency, the calculations performed at 20 bar turbine inlet condition. Results showed that as mixture strength increases the net electric power increases, where the cycle thermal efficiency decreases. The increase in NH_3/H_2O mixture strength from 0.87 to 0.9 causes the net electrical power output to increase by about 17%.

As per geothermal working fluid temperature, Figure 6 shows the effect of geothermal working fluid temperature on heat transfer area. Results show that as working fluid temperature increases, heat transfer area for condenser increases, where the heat transfer area for the evaporator sharply decreases.

Figure 7 shows the effect of geothermal working fluid temperature on net electrical power. It is obvious that as the geothermal working fluid temperature increases, the net electrical power increases. Results showed that when working fluid increases from 100 to 120 C, the net electric power increases by about 30%. Figure 8 showed the net electric power and thermal efficiency for conventional Rankine cycle operating at the same conditions.

In this research calculations been carried out to present mass flow rate, rate of energy, exergy and rate of exergy at different cycle nodes, Table 3. Results show how the NH_3/H_2O mixture strength varies across the cycle, another observation that rate of energy and exergy values reach a maximum value at turbine inlet.

Table 4 shows the exergy destruction per component, results shows that the highest value of exergy destruction occurs in the turbine (383.9 kW) which represents 70.39% of total cycle exergy destruction, followed by the evaporator with a value of 70.29 kW exergy destruction, which represents 19.89% of total exergy destruction. Table 3 also shows that the components with low exergy destruction are the condenser and the separator.

VI. CONCLUSIONS

Geothermal energy is an interesting type of thermal energy to produce electrical energy. The present research investigates the feasibility of utilizing low enthalpy geothermal energy using Kalina cycle. It is realized that the Kalina cycle has an advantage of other technological advances. Based on numerical calculations and in terms of first and second laws of thermodynamics, the following conclusions, which show a high improvement potential, can be drawn:

As NH_3/H_2O mixture strength increases, both heat transfer area for condenser and evaporator are increases, and the required heat transfer area for the condenser is greater than the evaporator at higher values of mixture strength.

The net cycle electrical power increases with the increase of NH_3/H_2O mixture strength.

As the geothermal working fluid temperature increases, the heat transfer area for evaporator decreases, hence, reducing production cost, where it shows an increase for the case of condenser.

The highest value of the exergy destruction occurred in the turbine followed by the evaporator, while the lowest value of exergy destruction occurs in the condenser and separator.

REFERENCES

[1]. Demirbaş, A. Global Renewable Energy Resources. Energy Sources. 2006; 28(8):779-792.
[2]. Holm, A., Blodgett, L., Jennejohn, D., & Gawell, K. (2010). Geothermal Energy: International Market Update. Geothermal Energy Association. 2010.
[3]. Kagel, A. The State of Geothermal Technology – Part II: Surface Technology. Geothermal Energy Association, Washington D.C. 2008.
[4]. Sanyal, S. K. Future of Geothermal Energy. Thirty-Fifth Workshop on Geothermal Reservoir Engineering, 1-3 Feb. 2010.
[5]. Lee, K. C. Classification of Geothermal Resources by Exergy. Geothermics, 2001; 30:431-442.
[6]. Web1. Geothermal energy overview 2010. http://www.ourenergy.com/news/geothermal_energy_overview_2010.html
[7]. Kreith, F. and Goswami, D. Y. Handbook of Energy Efficiency and Renewable Energy. CRC Press, Taylor & Francis Group. 2007.
[8]. Padilla, R. V., Demirkaya, G., Goswami, D. Y., Stefanakos, E., & Rahman, M. M. Analysis of power and cooling cogeneration using ammonia-water mixture. Energy, 2010; 35(12): 4649-4657.
[9]. Lolos, P. A. Thermodynamic Analysis of a Kalina Power Unit Driven by Low Temperature Heat Source. Thermal Science, 2009; 13(4): 21-31.
[10]. Koroneous, C. J., and Rovas, D. C. Electricity From Geothermal Energy with the Kalina Cycle - An Exergy Approach. IEEE, 2007;423-428.
[11]. Rogdakis, E. D. Thermodynamic Analysis, Parametric Study and Optimum Operation of the Kalina Cycle. International journal of energy research, 1996; 20:359-370.
[12]. Marston, C. H., and Hyre, M. Gas Turbine Bottoming Cycles: Triple-Pressure Steam Versus Kalina. Journal of Engineering for Gas Turbines and Power - ASME Trans., 1995;117: 10-15.
[13]. Park, Y. M., and Sonntag, R. E. A Preliminary Study of the Kalina Power Cycle in Connection with a Combined Cycle System. International journal of Energy Research, 1990; 14: 153-162.
[14]. Murugan, R. S., and Subbarao, P. M. Thermodynamic Analysis of Rankine-Kalina Combined Cycle. Int. J. of Thermodynamics. 2008; 11(3):133-141.
[15]. Murugan, R S, and Subbarao, P. M. V. Efficiency enhancement in a Rankine cycle power plant: combined cycle approach. Proceedings of the Institution of Mechanical Engineers, Part A: Journal of Power and Energy, 2008; 222(8):753-760.
[16]. Marston, C. H. Parametric Analysis of the Kalina Cycle. Journal of Engineering for Gas Turbines and Power - ASME Trans., 1990; 112:107-116.
[17]. Lu, S., and Goswami, D. Y. Theoretical Analysis of Ammonia-Based Combined Power/Refrigeration Cycle at Low Refrigeration Temperatures. Proceedings of solar 2002 sunrise on the reliable energy economy, Reno, Nevada.
[18]. Nasruddin, Usvika, R., Rifaldi, M., & Noor, A. Energy and exergy analysis of kalina cycle system (KCS) 34

with mass fraction ammonia-water mixture variation. Journal of Mechanical Science and Technology, 2009; 23(7):1871-1876.

[19]. Lolos, P. A., and Rogdakis, E. D. A Kalina power cycle driven by renewable energy sources. Energy, 2009; 34(4):457-464.

[20]. Valdimarsson, Pall and Eliasson, L. Factors Influencing the Economics of the Kalina Power Cycle and Situation of Superior Performance. International Geothermal Conference, Reykjavik. 2009; 32-40.

[21]. Dejfors, C., and Svedberg, G. Second Law Analysis of Ammonia-Water Power Cycle for Direct-Fired Cogeneration Applications. Int. J. Applied Thermodynamics, 1999; 2(3):125-131.

[22]. Vidal, A., Best, R., Rivero, R., & Cervantes, J. Analysis of a combined power and refrigeration cycle by the exergy method. Energy, 2006; 31(15):3401-3414.

[23]. Maack, R., and Valdimarsson, P. Operating Experience with Kalina Power Plants. In: Geothermische Stromerzeugung Stand der Technik und Perspektiven, Potsdam 17/18. Oktober, 2002.

FIGURES

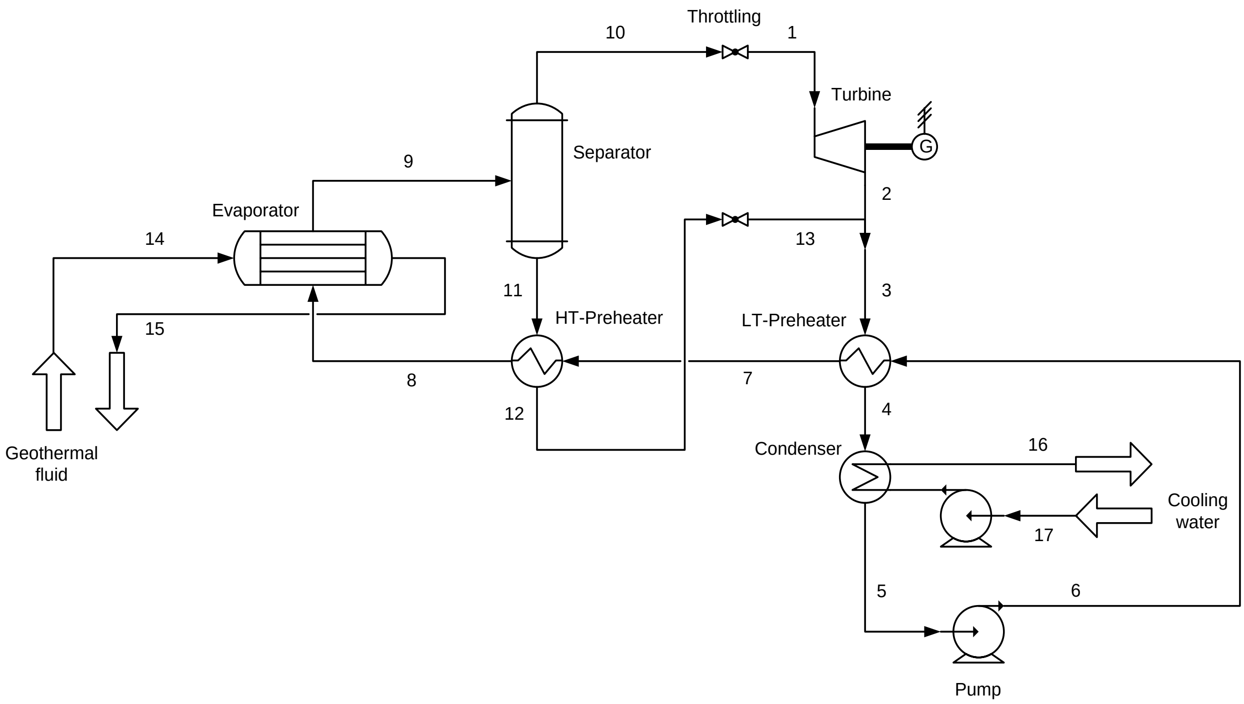

Fig 1:- Kalina Cycle Schematic Diagram

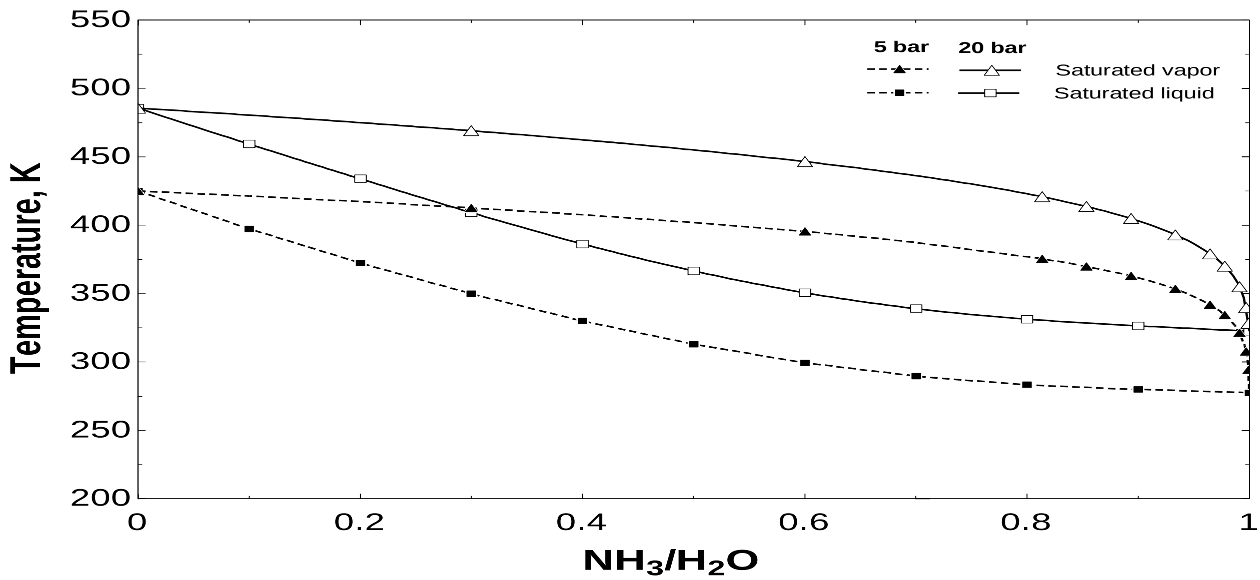

Fig 2:- Phase Diagram for Ammonia Water Mixture

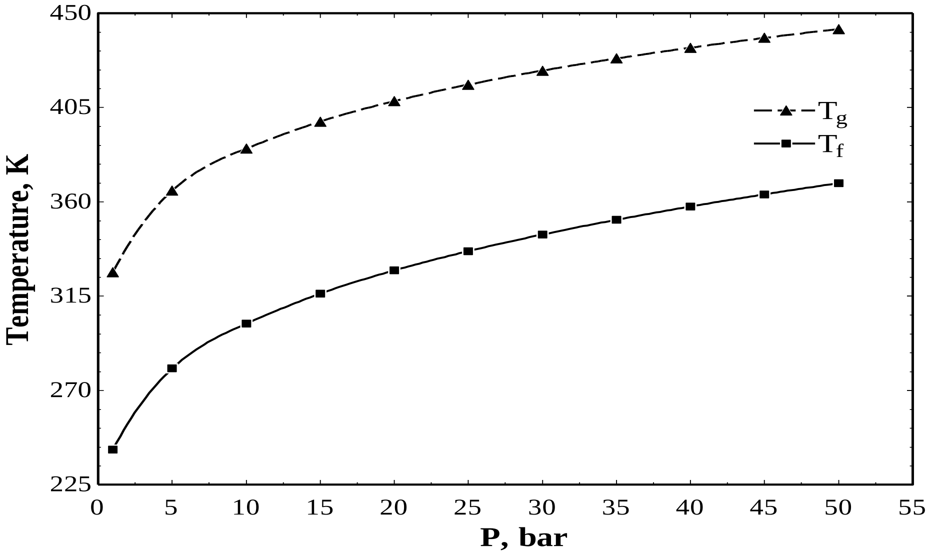

Fig 3:- The effect of ammonia water mixture pressure on saturation temperatures

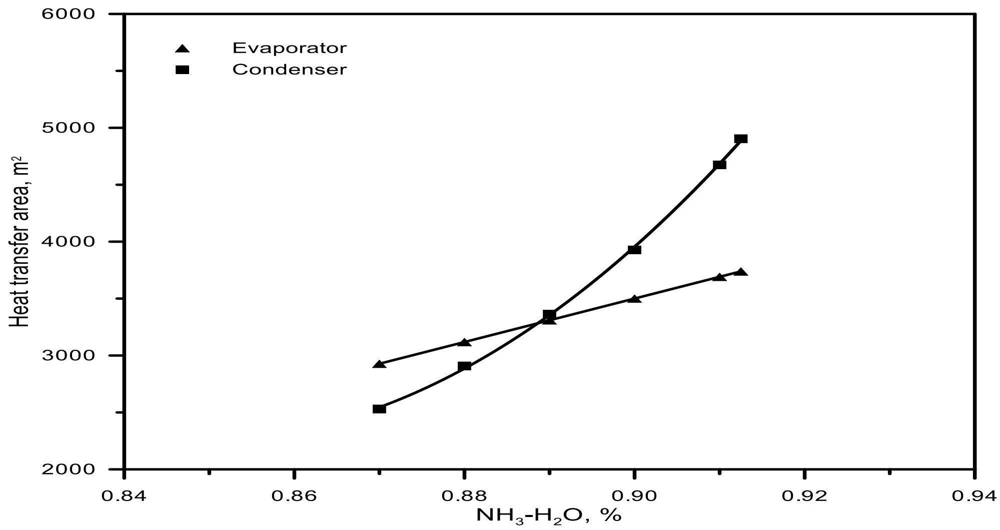

Fig 4:- The effect of ammonia water mixture strength on evaporator and condenser heat transfer area

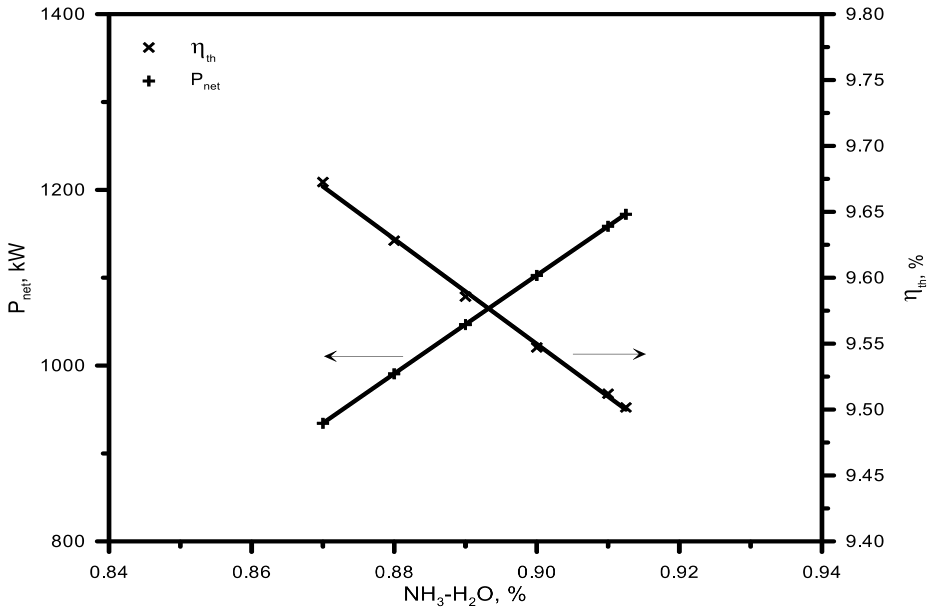

Fig 5:- The effect of ammonia water mixture strength on net power output and thermal efficiency

ISSN No:-2456-2165

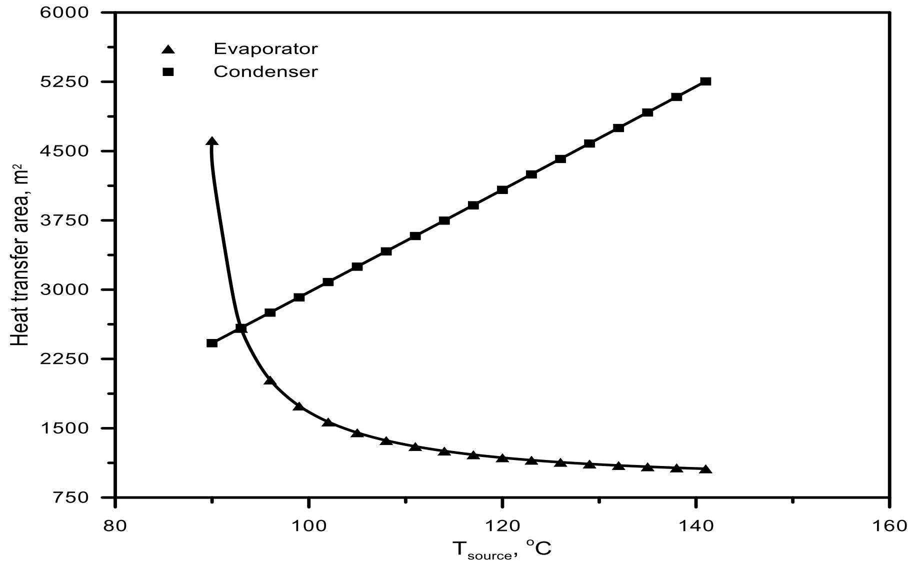

Fig 6:- Effect of geothermal source temperature on evaporator and condenser heat transfer area

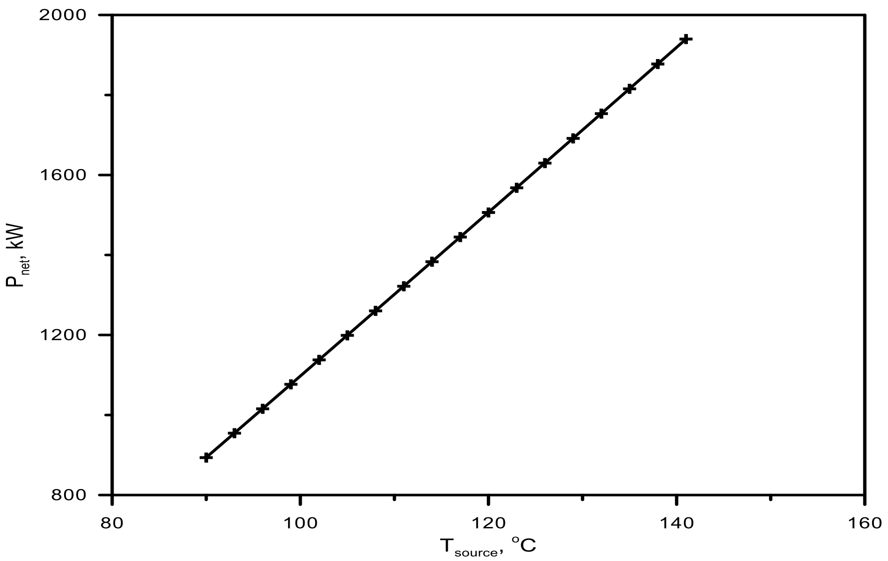

Fig 7:- The effect of geothermal source temperature on net power output

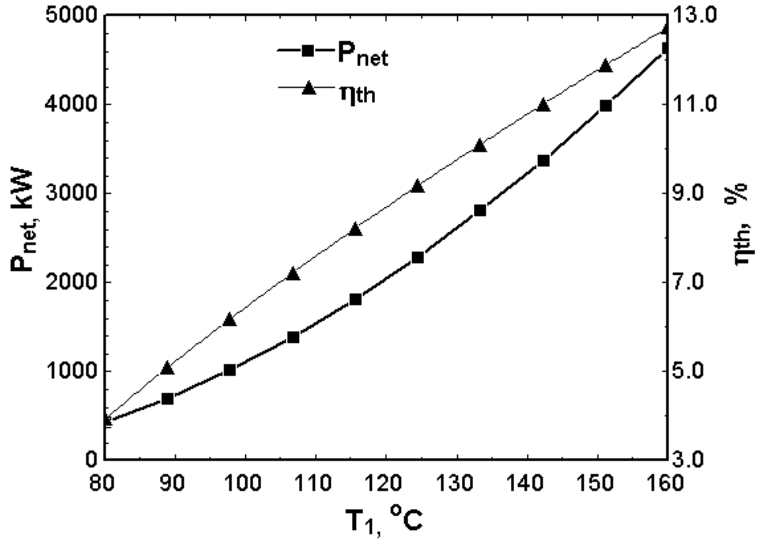

Fig 8:- The effect of inlet temperature on net power output and thermal efficiency for a conventional Rankine cycle

TABLES

Country	Installed Capacity (MW)	Rank
United States	3,086	1
Philippines	1,904	2
Indonesia	1,197	3
Mexico	958	4
Italy	843	5
New Zealand	628	6
Iceland	575	7
Japan	536	8
El Salvador	204	9
Kenya	167	10
Costa Rica	166	11
Nicaragua	88	12
Russia	82	13
Turkey	82	14
Papua New Guinea	56	15
Guatemala	52	16
Portugal	29	17
China	24	18
France	16	19
Ethiopia	7.3	20
Germany	6.6	21
Austria	1.4	22
Australia	1.1	23
Thailand	0.3	24

Table 1:- Countries generating geothermal power in 2010 (Holm et al., 2010)

TABLE I. KALINA CYCLE MODEL

Turbine

$P_{tur} = \dot{m}_{10}\left(h_{10} - h_2\right)$

$\eta_t = \dfrac{h_{10} - h_2}{h_{10} - h_{2s}}$

$ExD = \dot{m}_1 e_1 - \dot{m}_2 e_2 - \dot{m}_1 w_{tur}$

Isentropic efficiency = 0.85

LT-Preheater

Energy balance

$\dot{m}_3\left(h_3 - h_4\right) = \dot{m}_7\left(h_7 - h_6\right)$

$ExD = \dot{m}_3 e_3 + \dot{m}_6 e_6 - \dot{m}_4 e_4 - \dot{m}_7 e_7$

Adiabatic, No pressure drop

Condenser

Energy balance

$Q_c = \dot{m}_4\left(h_4 - h_5\right) = \dot{m}_{17}\left(h_{16} - h_{17}\right)$

Heat transfer area

$Q_c = A_{cond} U_c \text{ LMTD}$

$$\text{LMTD} = \frac{\Delta t_{in} - \Delta t_{out}}{\ln\left(\Delta t_{in} / \Delta t_{out}\right)}$$

$ExD = \dot{m}_{18} e_{18} + \dot{m}_4 e_4 - \dot{m}_5 e_5 - \dot{m}_{16} e_{16}$

No pressure drop, Overall heat transfer coefficient is constant, $U_c = 1.1\,\text{kW/m}^2\text{K}$

HT-Preheater

Energy balance

$\dot{m}_{11}\left(h_{11} - h_{12}\right) = \dot{m}_7\left(h_8 - h_7\right)$

$ExD = \dot{m}_{11} e_{11} + \dot{m}_7 e_7 - \dot{m}_{12} e_{12} - \dot{m}_8 e_8$

Adiabatic, No pressure drop

Evaporator

Energy balance

$Q_e = \dot{m}_{14}\left(h_{14} - h_{15}\right) = \dot{m}_8\left(h_9 - h_8\right)$

Heat transfer area

$Q_e = A_{evap} U_e \text{ LMTD}$

$$\text{LMTD} = \frac{\Delta t_{in} - \Delta t_{out}}{\ln\left(\Delta t_{in} / \Delta t_{out}\right)}$$

$ExD = \dot{m}_{14} e_{14} + \dot{m}_8 e_8 - \dot{m}_9 e_9 - \dot{m}_{15} e_{15}$

No pressure drop, Overall heat transfer coefficient is constant, $U_e = 1.1\,\text{kW/m}^2\text{K}$

Separator

Total mass balance

$\dot{m}_9 = \dot{m}_{10} + \dot{m}_{11}$

NH_3 mass balance

$z_9.\dot{m}_9 = z_{10}.\dot{m}_{10} + z_{11}.\dot{m}_{11}$

$P_9 = P_{10} = P_{11}$

$T_9 = T_{10} = T_{11}$

Energy balance

$h_9.\dot{m}_9 = h_{10}.\dot{m}_{10} + h_{11}.\dot{m}_{11}$

$ExD = \dot{m}_9 e_9 - \dot{m}_{10} e_{10} - \dot{m}_{11} e_{11}$

Adiabatic, No pressure drop

All components

Exergy

$e = h - h_0 - T_o(s - s_o)$

Chemical exergy neglected

State	Z	T °C	P bar	H kJ/kg	S kJ/kg.K	Flow rate kg/s	Rate of Energy kW	Specific Exergy kJ/kg	Rate of Exergy kW
1	0.985	88.72	19.80	1771.52	5.935	7.16	12684.08	299.45	2144.04
2	0.985	28.46	5.00	1624.58	6.101	7.16	11631.99	104.70	749.65
3	0.870	33.41	5.00	1245.95	4.864	9.50	11836.53	82.33	782.09
4	0.870	20.00	4.98	1140.65	4.516	9.50	10836.18	77.25	733.87
5	0.870	7.14	4.88	231.43	1.329	9.50	2198.59	85.89	815.91
6	0.870	7.63	21.50	234.90	1.333	9.50	2231.55	88.20	837.93
7	0.870	29.85	21.00	340.20	1.694	9.50	3231.90	89.54	850.58
8	0.870	42.92	20.50	403.50	1.899	9.50	3833.25	93.80	891.05
9	0.870	89.00	20.00	1419.96	4.923	9.50	13489.62	239.34	2273.76
10	0.985	88.72	20.00	1770.0	5.931	7.16	12673.20	299.08	2141.41
11	0.518	89.00	20.00	346.12	1.842	2.34	809.92	52.83	123.63
12	0.518	35.54	19.80	89.45	1.076	2.34	209.31	16.77	39.24
13	0.518	35.75	5.00	89.45	1.082	2.34	209.31	15.04	35.20
14	-	92.00	4.00	385.63	1.220	50.00	19281.50	46.17	2308.5
15	-	45.92	2.00	192.41	0.650	50.00	9620.50	17.11	855.50
16	-	20.00	2.00	84.11	0.300	137.97	11604.66	9.61	1325.89
17	-	5.00	2.00	21.22	0.080	139.97	2970.16	10.08	1410.90

Table 2:- Flow rate, rate of energy, exergy and rate of exergy at different cycle states.

Component	Rate of Exergy Destruction, kW	%
Turbine	383.90	70.39
LT-Preheater	35.57	6.52
HT-Preheater	43.92	8.05
Evaporator	70.29	12.89
Separator	8.73	1.60
Condenser	2.96	0.54

Table 3:- Exergy destruction of the cycle components